Experimental Investigation and Analytical Modeling of Prefabricated Reinforced Concrete Sandwich Panels

D.A. Bournas
European Commission, JRC, IPSC, European Laboratory for Structural Assessment (ELSA), Ispra, Italy.

G. Torrisi & F. Crisafulli
University of Cuyo, Mendoza, Argentina

A. Pavese
University of Pavia, Italy

SUMMARY:
The behavior of prefabricated reinforced concrete sandwich panels (RCSPs) was investigated experimentally and analytically in this study. Initially, tests were carried out on single full-scale RCSPs with or without openings, reproducing the behavior of lateral resisting cantilever and fixed-end walls. The performance and failure mode of all panels tested revealed coupling between the flexure and shear response. However due to their well-detailed reinforcement, all panels exhibited a relatively gradual strength and stiffness degradation and did not suffer from sudden shear failure. Then, an analytical column model was developed for the analysis of the walls' nonlinear response under cyclic loading. The model consists of an elastic bar with nonlinear flexural and shear springs concentrated at the column ends. It was concluded that this simple model represents very satisfactory effects of flexural and shear forces in the global response of the walls. The agreement of the proposed model with experimental response characteristics was quite good when the proper constitutive law were used.

Keywords: Prefabricated structures; RC walls; Seismic Behaviour, Interaction model

1. INTRODUCTION

After the excellent seismic performance of buildings constructed incorporating structural walls (Wood et al. 1987, Fintel 1995), in very strong earthquakes [e.g. in Chile, 1985 and Kocaeli (Turkey) 1999], there is presently a tendency to acknowledge similar q-factor values for frame and wall systems. In addition, during the 1988 Armenia earthquake poorly designed and constructed buildings that incorporated precast concrete walls as the main lateral force resisting system performed substantially better than buildings built with other structural systems (Wyllie 1989).

Although the use of precast structural walls in seismic areas of the world has been proved a cost-effective way for lateral resistance of buildings, the very big majority of structures are constructed with cast in place reinforced concrete (RC). During the past 15 years or so, however, the research community has increasingly focused on the use of precast concrete walls as the primary lateral load-resisting system in seismic regions (e.g. Kurama et al. 1999, Rahman and Restrepo 2000, Crisafulli et al. 2002, Holden et al. 2003, Perez et al. 2003). The precast concrete structural walls systems, which have been investigated up to date, are generally arranged to provide lateral force resistance by cantilevering from the foundation structure, through coupling with beams or other special devices and by rocking about their foundation. Moreover structural wall systems showing strong non-linear response can be grouped into either equivalent monolithic or jointed systems. An analytic review of the precast structural wall systems can be found in a recent bulletin of fib (2003).

In this paper the seismic performance of an innovative prefabricated equivalent monolithic structural system comprising large RC sandwich panels (RCSPs) is investigated. Despite the use of prefabricated RCSPs have been introduced in the construction industry for more than 40 years (PCI 1997), the last have been used in practice primarily as gravity load bearing structural elements. More

recently, in the last decade, many companies from the international precast construction industry have started manufacturing RCSPs commercially with the aim of developing a quick and permanent building system which is supplemented with a satisfactory earthquake resistance. Consequently the investigation of the seismic performance of prefabricated RCSPs still remains a challenging task, which is addressed in this study experimentally and analytically. In the present study the authors investigate experimentally the behavior of prefabricated RCSPs under simulated seismic loading through a large experimental campaign. In addition, an analytical column model was developed for the analysis of the walls' nonlinear response under cyclic loading

1.1. Description of the structural system

A RCSP is composed of an Expanded Polystyrene (EPS) foam core with prefabricated galvanized steel wire mesh reinforcement encased in two layers of sprayed concrete on both sides, as shown in Fig. 1a. The steel wire mesh of reinforcement mounted on each face of the polystyrene foam is drawn with hot galvanization and consists of 2.5 mm and 3.5 mm diameter horizontal and longitudinal reinforcement, respectively, spaced at 65 mm; this gives a longitudinal reinforcement ratio of 0.42%, which is more than the minimum longitudinal reinforcement of 0.2% of the Eurocode. The connection between the two concrete layers through the core of the wall panel is secured with 3 mm diameter steel connectors welded to the front and back wire meshes through the polystyrene. These connectors ($\sim 80/m^2$) could be straight or inclined depending on the manufacturing plan. The uniform connection between the parts of the sandwich panel is also favored by the surfaces of the polystyrene which have been initially corrugated. The panels considered in this study have depth and length of corrugation equal to 10 mm and 70 mm, respectively (Fig. 1a). In this way the assembly develops nearly full composite behavior in stiffness and shear transfer.
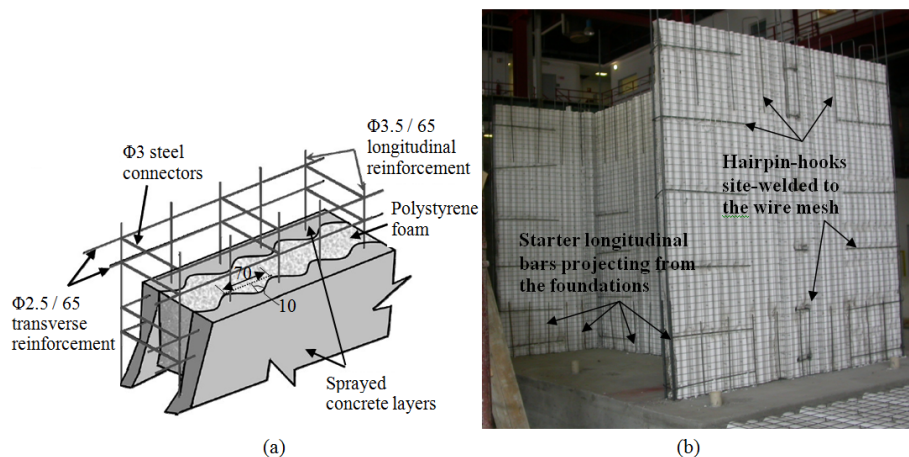

Figure 1. (a) Detail of a typical RCSP. (b) Connection between RCSPs

Each type of steel wire meshes used (horizontal, longitudinal, connector ties) has a nominal yield stress of 600 MPa. The shotcrete has typically a thickness of 35 mm (also greater values could be considered) and a characteristic 28 days cube compressive strength higher than 25 MPa. It should be noted that in order to control shrinkage a fiber-reinforced concrete could be used. Connection between the panels and the foundation or floor is made by means of starter steel bars projecting from the foundation (or floor) as shown in Fig. 1b. In the present study, the transfer of the tensile forces from the panels to the foundation was made by 8 mm diameter deformed bars which were placed at distances of 300 mm. These bars had a yield stress of 550 MPa. Typical characteristics of low-rise buildings constructed with this construction system comprise 1-5 stories with 3 m height and typical span of the walls 3-5 m. The wall thickness ranges from 150 mm to 200 mm depending on the thickness of the EPS foam, while the density of the sandwich panel may be varying between 0.9-1.1 t/m^3. The fundamental period of vibration for a characteristic 3-storey building of this type is low, and in general does not exceed 0.2 sec, if full fixity at the base is assumed.

2. EXPERIMENTAL INVESTIGATION

2.1. Experimental Program

Initially a total of 4 full-scale RC panel specimens were constructed and tested under cyclic uniaxial flexure with constant axial load (Pavese and Bournas 2011). The specimens were constructed with stiff top and bottom beams. The top beam served to distribute the horizontal and axial loads to the wall while the bottom beam, clamped to the laboratory strong floor, simulated a rigid foundation. The geometries of the single storey structural panels are shown in Fig. 2 whereas their reinforcing details were identical to the precast RCSP described previously. These specimens were designed such that the effect panel length and level of the axial load on their seismic behavior could be investigated. In brief, the notation of panels is PL_A, where the letter P denotes the panel specimen, L defines the panel length (3 m or 4m) and A denotes the level of the applied axial load during test (150 kN or 300 kN). The panels were subjected to lateral cyclic loading which consisted of successive cycles progressively increasing in each direction, according to predefined drifts ratios which were equal to 0.1%, 0.2%, 0.4%, 0.6% and 1%. The loading protocol consisted of three cycles at each level of displacement. At the same time a constant axial load was applied to the panels corresponding approximately to 2.5% and 5% of their compressive strength, which was calculated by multiplying the gross section of concrete area (not the EPS core) by the average compressive strength of all tested panels.
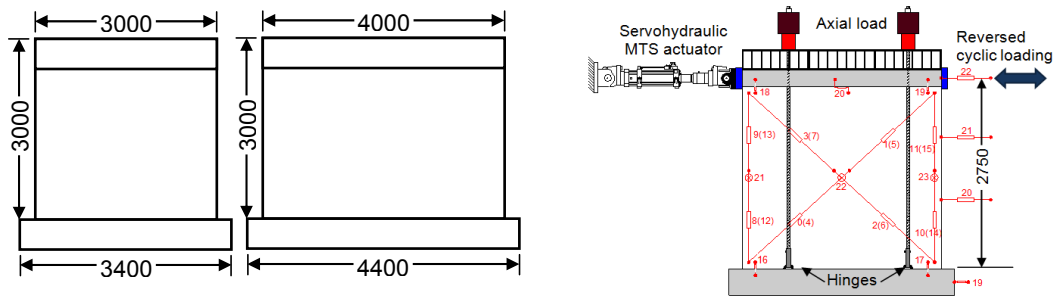

Figure 2. (a) Geometry of the panels (Dimensions in mm). (b) Schematic of test set up and instrumentation

2.2. Experimental Results

The response of all panels tested is given in Fig. 3 in the form of load-drift ratio loops. Key results about panels' general behaviour are also summarized in Table 1. They include: (a) The peak resistance in the two directions of loading. (b) The drift ratio corresponding to panels' yielding θ_y in the two directions of loading. The displacement at panels' yielding was calculated with a bi-linearization of the experimental load-displacement curve following the procedure proposed by FEMA. (c) The drift ratio corresponding to peak resistance in the two directions of loading. (d) The drift ratio at conventional "failure" of the wall θ_u, defined as reduction of peak resistance in a cycle below 80% of the maximum recorded resistance in that direction of loading. (e) The behaviour factor q, which is defined as $q=\mu_\theta=\theta_u/\theta_y$, where θ_y and θ_u are the average (in both directions of loading) drift ratios of the panel at yield and at failure, respectively.

Table 2.1. Summary of test results.

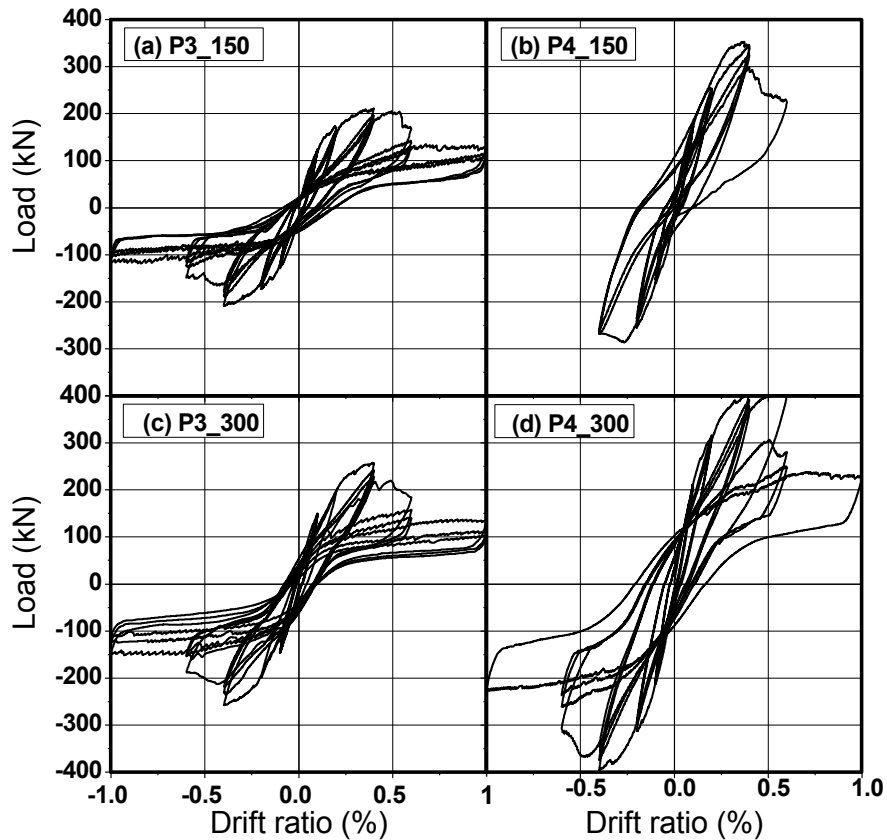| Specimen notation	Peak force (kN)		Drift at Yielding, θy (%)		Drift at peak force (%)		Drift at "failure" θu (%)		Displacement ductility factor $\mu_\Delta = \theta_u / \theta_y$
	Push	Pull	Push	Pull	Push	Pull	Push	Pull	
P3_150	211.4	-208.9	0.19	0.17	0.39	-0.40	0.60	-0.44	2.88
P3_300	-257.9	257.4	0.15	0.18	0.39	-0.40	0.51	-0.49	3.03
P4_150	352.9	-286.5	0.24	0.19	0.37	-0.27	0.42	--	2.01
P4_300	409.8	-396.5	0.23	0.20	0.40	-0.40	0.65	-0.57	2.84

Figure 3. Load versus drift ratio curves for all panels tested.

For all panels tested (P3_150, P3_300, P4_150, P4_300), significant longitudinal and horizontal tensile cracks were developed close to the regions of maximum moment and shear cracks parallel to the compression strut (Fig. 4a) at a drift ratio of about 0.4%, corresponding to peak lateral load. In the next loading cycle, corresponding to a drift ratio of 0.6%, the concrete under compression spalled and longitudinal bars buckled (Fig. 4b) along the lower (approximately) 100 mm from the base of panels corners, leading to substantial lateral strength degradation after peak lateral load. It is worth mentioning here that bar buckling at wall end sections could be prevented by providing adequate confinement to these sections, which may be achieved by hoops around boundary elements engaging vertical bars.

(a)   (b)

Figure 4. (a) Horizontal, vertical and shear cracking at peak lateral load. (b) Disintegration of concrete and bar buckling at the base of panels.

3. ANALYTICAL MODEL

3.1. Description of the macro-element column model

A column model was developed to take into account the bending and shear effects on RC columns. The model is a Euler-Bernoulli beam with shear deformations. This formulation takes into account the flexural and shear deformations of the element and does not possess the inadequacies of Timoshenko beams for large relations of L_s/d (Torrisi 2012). The element has also two nonlinear flexural springs at its ends as shown in Fig. 5. The nonlinear behaviour in shear is considered by degrading the stiffness of the element and is represented by two shear springs concentrated again at the ends of the element. Due to the fact that the model takes into account shear deformations, it can be used to represent the behaviour of shear critical RC members like shear walls or RCSPs.
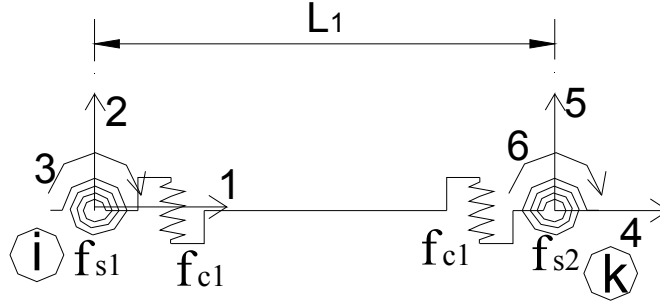

Figure 5. Beam-column element with nonlinear springs and degrees of freedom.

Each node of the element has 3 degrees of freedom (DOF), two translations about the orthogonal axes 1 and 2, and a rotation about the third axis 3, as it is illustrated in Fig. 5. The interaction between bending and shear forces is not directly taken into account, however these effects are coupled in the stiffness matrix of the element through the equilibrium.

3.2. Formulation of the macro-element model

The formulation of the macro-element is made in terms of flexibility. Due to the fact that the bending and shear springs are in series with the elastic beam (Fig. 5), the flexibility matrix of the element is the sum of the flexibility matrix of the springs and the beam, (Flores-Lopez 1993, D'ambrisi and Filippou 1999, Leu and Cheng 2000, Al-Haddad 1990, Thomson and Flores-Lopez 2004, Filippou and Issa 1998, Torrisi, 2012). The flexibility matrix for the elastic beam, nonlinear flexural springs and shear effects are presented in equation 3.1.

$$[F_{eb}] = \begin{bmatrix} \dfrac{L_1}{EA} & 0 & 0 \\ 0 & \dfrac{L_1}{3EJ} & -\dfrac{L_1}{6EJ} \\ 0 & -\dfrac{L_1}{6EJ} & \dfrac{L_1}{3EJ} \end{bmatrix} \quad , \quad [F_{ec}] = \begin{bmatrix} 0 & 0 & 0 \\ 0 & \dfrac{1}{GA_cL_1} & \dfrac{1}{GA_cL_1} \\ 0 & \dfrac{1}{GA_cL_1} & \dfrac{1}{GA_cL_1} \end{bmatrix} \quad , \quad [F_{bil}] = \begin{bmatrix} 0 & 0 & 0 \\ 0 & f_{s1} & 0 \\ 0 & 0 & f_{s2} \end{bmatrix} \quad , \quad [F_{ci}] = \begin{bmatrix} 0 & 0 & 0 \\ 0 & f_{ci} & f_{ci} \\ 0 & f_{ci} & f_{ci} \end{bmatrix} \quad (3.1)$$

where F_{eb}, F_{ec}, F_{bil}, F_{ci} are the flexibility matrices for the elastic bending part, elastic shear, nonlinear flexural springs and nonlinear shear behaviour, respectively. The L_1, A, A_c, J, E, G, are the length, cross sectional area, shear area, moment of inertia of the section, elastic modulus and shear modulus of the element, respectively. The nonlinear flexural flexibility is given by f_{s1} and f_{s2} and the nonlinear shear flexibility is f_{ci}, where the expressions for these flexibilities are given in equation 3.2 (Carr, 2007).

$$f_{si} = \frac{(1-r_i)}{r_i} \frac{L_p}{EJ} \qquad\qquad f_{ci} = \frac{(1-p_i)}{p_i} \frac{1}{GA_cL_1} \left(\frac{L_{cr}}{L_1} \right) \alpha_c \qquad\qquad (3.2)$$

In equation 3.2, r_i and p_i are the slopes in the moment-curvature and shear force-shear strain relationships, respectively, whereas L_p is the plastic hinge length, L_{cr} is the length of the element with shear cracking (generally $L_{cr}=L_1$) and finally α_c is a factor to match the experimental results. The value of α_c is given by the following relationship:

$$\alpha_c = 12 \frac{G}{E} \frac{L_1^2}{d^2} \tag{3.3}$$

The column flexibility matrix is $F = F_{eb} + F_{ec} + F_{bil} + F_{ci}$ and the elemental stiffness matrix is the inverse of F ($K_o = F^{-1}$). By using the flexibility matrix of the element it is possible to obtain its stiffness matrix and then to add it to the stiffness of the structure. The total stiffness matrix for the column, K_e, is given by Eq. 3.4:

$$[K_e] = [B]^T [K_o][B] \tag{3.4}$$

Where B is a transformation matrix defined by Eq. 3.5:

$$[B] = \begin{bmatrix} 1 & 0 & 0 & -1 & 0 & 0 \\ 0 & 1/L_1 & 0 & 0 & -1/L_1 & 1 \\ 0 & 1/L_1 & 1 & 0 & -1/L_1 & 0 \end{bmatrix} \tag{3.5}$$

3.3. Solution procedure

The solution is made by increments of loads or displacements and in each increment the nodal displacements and rotations are calculated. The vector Δu in Eq. 3.6 represents the incremental node displacements in the element. The subscript 1 and 2 are related to the initial and end nodes of the element.

$$\{\Delta u\} = \begin{bmatrix} \Delta x_1 & \Delta y_1 & \Delta \theta_1 & \Delta x_2 & \Delta y_2 & \Delta \theta_2 \end{bmatrix}^T \tag{3.6}$$

By multiplying $\boldsymbol{K_e}$ (Eq. 3.4) with the increment of displacements Δu (Eq. 3.6), the increment of internal forces ΔQ (Eq. 3.7) matrix is obtained.

$$\{\Delta Q\} = \begin{bmatrix} \Delta N_1 & \Delta V_1 & \Delta M_1 & \Delta N_2 & \Delta V_2 & \Delta M_2 \end{bmatrix}^T \tag{3.7}$$

Afterwards, the increments in curvatures ($\Delta\phi_m$) and shear strain ($\Delta\gamma$) are calculated by using Eq. 3.8 (Carr, 2007; Torrisi, 2012). With these values the instantaneous stiffness and forces (and moments) are calculated by making use of the proper moment-curvature and shear forces-shear strains relationships (which should be given).

$$\Delta\phi_m = \frac{\Delta M_m}{r_m EJ} \qquad \Delta\gamma = \frac{\Delta M_i + \Delta M_k}{p\ GA_c} = \frac{\Delta V}{p\ GA_c} \tag{3.8}$$

where ΔM_m and ΔV are the moment and shear forces increments. The global solution can be derived on an explicit algorithm with no need for iteration to check convergence. Alternatively, an implicit algorithm can be used, where the Newton-Raphson iteration procedure is needed to achieve convergence in each time step. In the next section, an explicit solution was used for the modelling of the RCSPs.

4. MODEL APPLICATION-VERIFICATION

The macro-element column model was applied for the analysis of the RCSPs nonlinear response. Figure 6 shows the generic envelopes used in the analysis. In the monotonic response, the moment-curvature and shear force-shear strain envelopes can have more than three branches to take into account the degradation of forces and moments due to the cyclic behaviour.
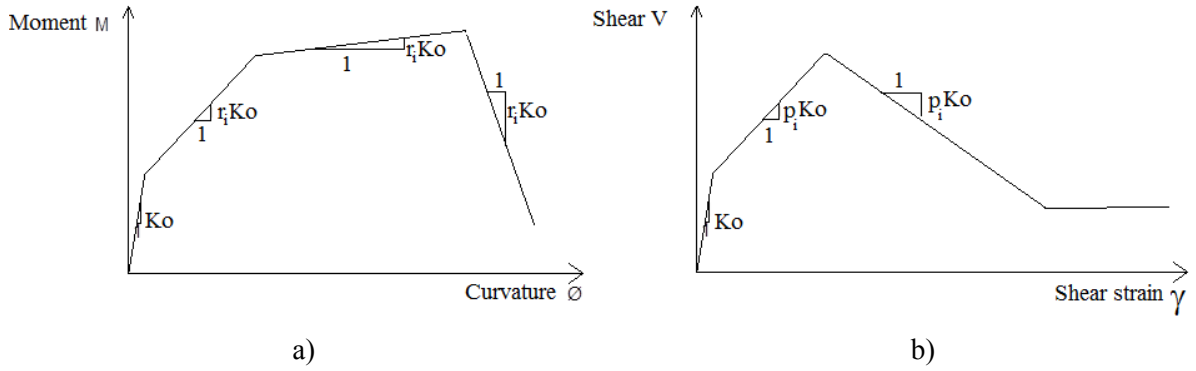

a)   b)

Figure 6. Generic envelopes used in the analysis: a)Moment-curvature, b)Shear force-shear strain
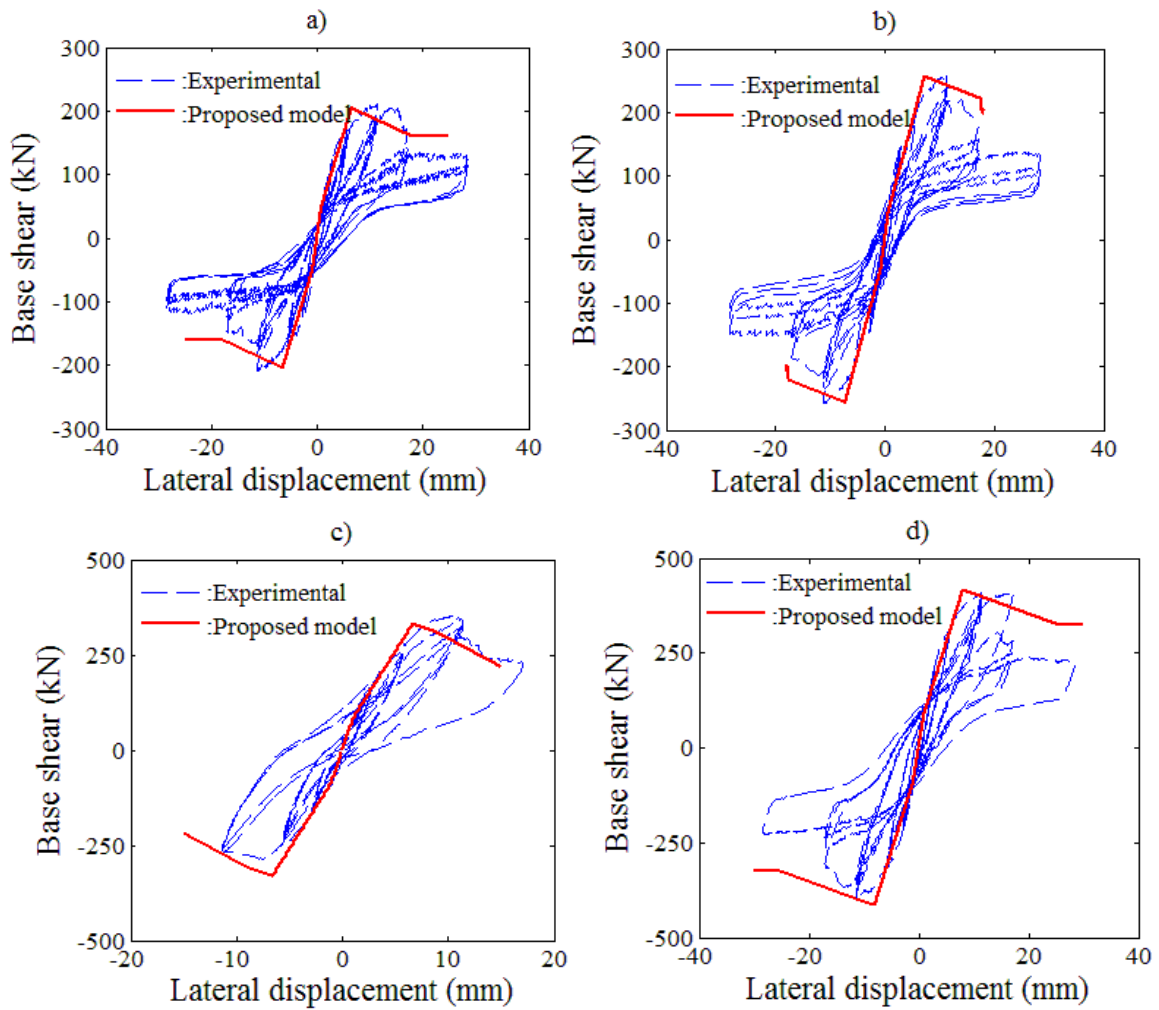

Figure 7. Comparison of experimental and analytical responses. a) P3_150, b)P3_300, c) P4_150, d)P4_300

Due to the effects of sliding and debonding of bars in the experimental program, and because the model implemented does not take into account that behaviour, only the monotonic envelope was computed and not the cyclic behaviour. Figure 7 presents the response of the four RCSPs (P3_150, P3_300, P4_150, P4_300) obtained with the proposed model for monotonic loading in the form of base shear-lateral displacement. In the same plot, the experimental base shear versus lateral displacement loops are reproduced to facilitate the comparison between model's prediction and actual response. Overall, it may be concluded that a good correlation between experimental an analytical results exists. The initial stiffness, peak force and stiffness degradation are well reproduced by the proposed model. On the basis of these (limited) results it seems that the good correlation between experimental an analytical results is independent of the axial load percentage (150 or 300 kN) and panel length (3 or 4 m).

5. CONCLUSIONS

In the present study the authors investigated experimentally the behavior of prefabricated RCSPs under simulated seismic loading through a large experimental campaign. Tests were carried out on single full-scale panels. From the results obtained in this study, the authors believe that, the presented structural system with prefabricated RCSPs comprise a promising construction system for regions of moderate and high seismicity.

Further an analytical column model was developed for the analysis of the walls' nonlinear response. The model consists of an elastic bar with nonlinear flexural and shear springs concentrated at the column ends. It was concluded that this simple model represents very satisfactory effects of flexural and shear forces in the global response of the walls. The agreement of the proposed model with experimental response characteristics was quite good when the proper constitutive law were used.

REFERENCES

Al-Haddad, M.S., (1990). Mathematical model for cyclic loading of a R.C. beam with relocatable plastic hinges. *Journal of King Soud University. Enginering Sciences* **2:2**, 213-228.
Carr, A., (2007). Ruaumoko theory and user manual. *University of Canterbury, New Zealand.*
Crisafulli, F. J., Restrepo, J. I. and Park, R. (2002). Seismic design of lightly reinforced precast rectangular wall panels. *PCI Journal.* **47: 4**, 104-121.
D'ambrisi, A. and Filippou, F.C., (1999). Modeling of cyclic shear behavior in RC members. *Journal of Structural Engineering.* **125:10**, 1143-1150.
Federation International du Beton – *fib* (2003). Seismic Design of Precast Concrete Buildings Structures. **Bulletin 27**, Lausanne.
Filippou, F.C, and Issa, A., (1988). Nonlinear analysis of reinforced concrete frames under cyclic load reversals. Report No. UCB/EERC–88/12, *Earthquake Engineering Research Center*. College of Engineering, University of California, Berkeley
Fintel M. (1995). Performance of buildings with shear walls in earthquakes in the last thirty years'' *PCI Journal.*, **4:3**,62-80.
Flores Lopez, J., (1993). Modelos de daño concentrado para la simulación numérica del colapso de pórticos planos. *Revista Internacional de Métodos Numéricos para Cálculo y Diseño en Ingeniería.* **9:2**, 123-139.
Holden, T., Restrepo, J. and Mander, J. B. (2003). Seismic Performance of Precast Reinforced and Prestressed Concrete Walls. *ASCE Journal of Structural Engineering.* **129:3**, 286-296.
Kurama, Y., Sause, R., Pessiki, S., and Lu, L.W. (1999). Lateral load behavior and seismic design of unbonded post-tensioned precast concrete walls. *ACI Structural Journal.* **96:4,** 622–632.
Leu, L.J. and Cheng, J.C., (2000). Flexibility based formulation for nonlinear analysis of reinforced concrete frames considering the effects of finite length inelastic zones. *Journal of the Chinese Institute of Engineers,* **23:1**, 97-108.
Pavese, A. and Bournas, D.A., (2011). Experimental Assessment of the Seismic Performance of a Prefabricated Concrete Structural Wall System. *Elsevier Engineering Structures*, **33:6**, 2049-2062
PCI Committee on Pre-cast Sandwich Wall Panels. (1997). State-of-the-art of precast/ pre-stressed sandwich wall panels. *PCI Journal.* **42:2**, 92–134.
Pérez, F. J., Pessiki, S., Sause, R., and Lu, L.-W. (2003). Lateral load tests of unbonded post-tensioned precast

concrete walls. *Special publication of large-scale structural testing, American Concrete Institute*, **SP 211-8** ,161–182.

Rahman, A. and Restrepo, J. I. (2000). Earthquake resistant precast concrete buildings: Seismic performance of cantilever walls prestressed using unbonded tendons. **Research Rep. No. 2000-5**. Dept. of Civil Engineering, Univ. of Canterbury, Christchurch, New Zealand.

Thomson, E. and Florez-Lopez, J., (2004). A simplified damage model for shear dominated reinforced concrete walls under lateral forces. *13th World Conference on Earthquake Engineering* , Vancouver, B.C., Canada.

Torrisi, G. (2012). Diseño y análisis de estructuras de hormigón armado y mampostería. *Tesis de doctorado 318p.* Facultad de Ingeniería, Universidad Nacional de Cuyo, Mendoza, Argentina, *(to be published)*.

Wood, S., Wright, J., and Moehle, J. (1987). The 1985 Chile earthquake, observations on earthquake-resistant construction in Vina del Mar. Civil Engineering Studies, **Structural Research Series No. 532**, Univ. of Illinois, Urbana, I11.

Wyllie, L. A, Jr., and Filson, J. R. (1989). Armenia earthquake reconnaissance report. *Earthquake Spectra Publication No. 89.01*. Special Supplement.